



Condition for sustained oscillations in repressilator based on a hybrid modeling of gene regulatory networks

Honglu Sun, Jean-Paul Comet, Maxime Folschette, Morgan Magnin

► To cite this version:

Honglu Sun, Jean-Paul Comet, Maxime Folschette, Morgan Magnin. Condition for sustained oscillations in repressilator based on a hybrid modeling of gene regulatory networks. International Conference on Bioinformatics Models, Methods and Algorithms (BIOINFORMATICS 2023), Feb 2023, Lisbon, Portugal. pp.29-40, 10.5220/0011614300003414 . hal-03902156

HAL Id: hal-03902156





<https://hal.science/hal-03902156>

Submitted on 15 Dec 2022

HAL is a multi-disciplinary open access archive for the deposit and dissemination of scientific research documents, whether they are published or not. The documents may come from teaching and research institutions in France or abroad, or from public or private research centers.

L'archive ouverte pluridisciplinaire **HAL**, est destinée au dépôt et à la diffusion de documents scientifiques de niveau recherche, publiés ou non, émanant des établissements d'enseignement et de recherche français ou étrangers, des laboratoires publics ou privés.

Condition for sustained oscillations in repressilator based on a hybrid modeling of gene regulatory networks

Honglu Sun¹^a, Jean-Paul Comet²^b, Maxime Folschette³^c and Morgan Magnin¹^d

¹Nantes Université, École Centrale Nantes, CNRS, LS2N, UMR 6004, F-44000 Nantes, France

²University Côte d’Azur, I3S laboratory, UMR CNRS 7271, CS 40121, 06903 Sophia Antipolis Cedex, France

³Univ. Lille, CNRS, Centrale Lille, UMR 9189 CRISTAL, F-59000 Lille, France

honglu.sun@ec-nantes.fr, Jean-Paul.Comet@univ-cotedazur.fr, maxime.folschette@centralelille.fr,
morgan.magnin@ec-nantes.fr

Keywords: Hybrid modeling, Repressilator, Sustained oscillation, Gene regulatory network, Synthetic biology.

Abstract: In this work, we study the existence of sustained oscillations in the “canonical” repressilator, a basic synthetic circuit of 3 genes leading to sustained oscillations. Previous works mostly used differential equations to study the repressilator. In our work, a pre-existing hybrid modeling framework of gene regulatory networks called HGRN is used to model this system. Compared to differential equations, dynamical properties of HGRNs are easier to prove theoretically due to its lower dynamical complexity. The objective of this work is to find conditions for the existence of sustained oscillations described by separable constraints on parameters. With such separable constraints, each parameter is constrained individually by an interval, which can provide useful information for the design of synthetic circuits. Our two major contributions are the following: firstly, we develop, by using the Poincaré map, a sufficient and necessary condition for the existence of sustained oscillations; then, based on this condition, we give a method using the range enclosure property of Bernstein coefficients to compute compatible separable constraints. By applying this method, we successfully obtain sets of conditions for the existence of sustained oscillations described as separable constraints.

1 INTRODUCTION

With the developments in the field of synthetic biology in the recent years, the construction of synthetic gene regulatory networks in living cells which satisfy certain properties becomes possible. Stable and controllable synthetic circuits could have potential medical applications. Mathematical modeling is one of the ways to guide the design of these synthetic circuits. The modeling of many different synthetic circuits have been studied in the literature (Chaves and Jong, 2021; Firippi and Chaves, 2020; Chaves and Gouzé, 2011; Buşe et al., 2010).

In this work, we focus on one class of synthetic circuit: the repressilators, which are gene regulatory networks consisting of at least one feedback loop, in which the expression of each gene inhibits the expression of the next gene in the loop leading to an oscilla-

tory behavior. Among different repressilators, in this work, we focus on the canonical repressilator with three components (see Figure 1). Our objective is to study the conditions for the existence of sustained oscillations in this network. Long term perspective application of sustained oscillations in a repressilator could be the treatment of diseases related to circadian rhythms, for instance, by allowing drug delivery at a particular pace.

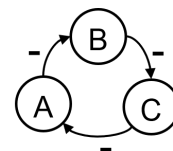






Figure 1: The influence graph of the canonical repressilator.

The existence of sustained oscillations in the repressilator has been studied both mathematically (Buşe et al., 2009; Buşe et al., 2010) and biologically (Potvin-Trottier et al., 2016; Elowitz and Leibler, 2000). In particular, the first biological implemen-

^a <https://orcid.org/0000-0002-8265-0984>

^b <https://orcid.org/0000-0002-6681-3501>

^c <https://orcid.org/0000-0002-3727-2320>

^d <https://orcid.org/0000-0001-5443-0506>

tation of the repressilator uses three natural repressor proteins, the TetR, LacI and CI repressors (Elowitz and Leibler, 2000).

In this work, we analyze mathematically the existence of sustained oscillations based on a pre-existing formalism, which has not yet been used for modeling the repressilator. In fact, how to biologically implement a repressilator with sustained oscillations is still an open question, particularly in eukaryotic cells, therefore exploring new models to search for conditions for sustained oscillations is of high interest.

Previous works about mathematical analysis of oscillations in the repressilator are mainly based on differential equations. Many models of the repressilator with three components are developed from a differential equation model using 6 variables (Elowitz and Leibler, 2000), with 3 variables for repressor-protein concentrations and 3 variables for corresponding mRNA concentrations. This 6-variable model can also be reduced to a 3-variable model with only repressor-protein variables under certain assumptions (Buşe et al., 2010). These models and their variations are extensively studied in the literature (Dukarić et al., 2019; Dilão, 2014; Kuznetsov and Afraimovich, 2012; Buşe et al., 2009; Müller et al., 2006; El Samad et al., 2005). One major limit about differential equations is that some dynamical properties are hard to analyze. Finally, let us mention some pre-existing tools that analyze dynamical properties on models such as GNA (De Jong et al., 2003) and RoVerGeNe (Batt et al., 2007), which are based mostly on qualitative properties.

In this work, a class of hybrid model called hybrid gene regulatory network (HGRN) (Behaegel et al., 2016; Cornillon et al., 2016) is used to model the repressilator. The HGRN is an extension of Thomas' discrete modeling framework (Thomas, 1973; Thomas, 1991). In HGRNs, the state space is separated into several discrete states, as for discrete models, and in each discrete state, the temporal derivative of the system is described by a constant vector making the system evolve continuously over time, as for differential equations. The most important property of HGRNs is that the "sliding mode" is allowed, which means that when a trajectory reaches a black wall (a boundary of the discrete state which cannot be crossed by trajectories) it is forced to move along the black wall.

There are two major reasons why we choose HGRNs to study synthetic circuits. Firstly, the dynamical complexity of HGRNs is lower than differential equations, making some dynamical properties of HGRNs easier to prove theoretically, such as the stability of limit cycles (Sun et al., 2022). Secondly,

from the parameters of a HGRN, we can easily derive the time required for the expression value of one gene to move from one threshold to another under certain regulation, and this information can be useful for the biological design of synthetic circuits.

The objective of this work is to find separable constraints on the parameters of a HGRN of the repressilator to ensure the existence of sustained oscillations. "Separable constraints on the parameters" means that the constraints are separable in a conjunction of constraints which cover a unique parameter each: each parameter is included individually in an interval. Thus we are looking for constraints which can be evaluated variable by variable. When all these constraints are satisfied, the global system shows the desired behavior. The reason why we choose constraints of separable form is that they can be easily interpreted and used. If such separable constraints can be found and if the individual intervals are not degenerated, the measure of the solution space is not null leading to a not null chance to be able to implement it in biological cells. These separable constraints represent a bounding box in the parameter space.

This work has the following contributions:

- It is the first study of sustained oscillations in the canonical repressilator based on HGRN.
- Similarly to the work (Sun et al., 2022), the Poincaré map is also used to analyze the stability of a certain cycle in HGRN. But contrary to (Sun et al., 2022) where the values of parameters are known, in this work, the Poincaré map is analyzed symbolically. By doing so, a sufficient and necessary condition for the existence of sustained oscillations in a HGRN of the canonical repressilator is proposed for the first time.
- An intermediate result implies some new control strategies for sustained oscillations in this HGRN of the canonical repressilator: controlling certain parameters such that their absolute values are sufficiently small compared to others.
- The range enclosure property of Bernstein coefficients, which can be used to over-approximate the image of a polynomial function on a bounding box, is adapted for the first time in this work to find bounding boxes in which all models satisfy certain conditions. Based on this method, some bounding boxes which only contain models with sustained oscillations are obtained.

The paper is organized as follows. In Section 2, the HGRN framework is defined and a HGRN of the canonical repressilator is introduced. In Section 3, we discuss different qualitative properties of this HGRN. In Section 4, the Poincaré map is used to compute a

sufficient and necessary condition for the existence of sustained oscillations. In Section 5, a method based on the range enclosure property of Bernstein coefficients is proposed to find separable constraints on parameters under which this HGRN has sustained oscillations. Finally, in Section 6, we make a conclusion and discuss our future works.

2 Modeling repressilator with HGRN

This section first defines a hybrid gene regulatory network (HGRN). Then a HGRN of the repressilator is introduced.

2.1 Hybrid gene regulatory network (HGRN)

Consider a gene regulatory network with N genes, the i^{th} gene has $n_i + 1$ discrete levels which are represented by integers: $\{0, 1, 2, \dots, n_i\}$. A discrete state s is obtained by attributing a valuation for each gene among its discrete levels. We denote d_s the integer vector which describes the discrete levels of all genes in s in order; in the following, for simplicity, we also call d_s a discrete state. The set of all discrete states is $E_d = \{d_s \in \mathbb{N}^N \mid \forall i \in \{1, 2, \dots, N\}, d_s^i \in \{0, 1, \dots, n_i\}\}$, where d_s^i is the i^{th} component of d_s . Based on the notion of discrete state, HGRNs are defined as follows:

Definition 1 (Hybrid gene regulatory network (HGRN)). A hybrid gene regulatory network (HGRN) is noted $\mathcal{H} = (E_d, c)$ where E_d is the set of all discrete states and c is a function from E_d to \mathbb{R}^N . For each $d_s \in E_d$, $c(d_s)$, also noted c_s , is called the celerity of discrete state d_s and describes the temporal derivative of the system in d_s .

In HGRNs, a hybrid state is used to fully describe the state of the system: it contains the discrete state in which the system currently is, and a fractional part that represents the (normalized) position of each variable inside this discrete state.

Definition 2 (Hybrid state of a HGRN). A hybrid state of a HGRN is a couple $h = (\pi, d_s)$ containing a fractional part π , which is a real vector in $[0, 1]^N$, and a discrete state d_s in E_d . E_h is the set of all hybrid states.

Unless there is an ambiguity, a hybrid state will be called simply a state. Based on this notion of state, a trajectory and a boundary are defined as follow.

Definition 3 ((Hybrid) trajectory). A (hybrid) trajectory τ is a function from a time interval $[0, t_0]$ to $E_\tau = E_h \cup E_{sh}$, where $t_0 \in \mathbb{R}^+ \cup \{\infty\}$, E_h is the set of all states, and E_{sh} is the set of all sequences of states ($E_{sh} = \{(h_0, h_1, \dots, h_m) \in (E_h)^{m+1} \mid m \in \mathbb{N} \cup \{\infty\}\}$).

A trajectory represents a simulation of the system over time. Consider a trajectory τ on $[0, t_0]$. For any $t \in [0, t_0]$, if $\tau(t) = (h_0, h_1, \dots, h_m) \in E_{sh}$, this means that there is a sequence of instant transitions at t , which begins from h_0 , reaches h_1 at first, then reaches h_2, \dots , and finally reaches h_m ; otherwise, if $\tau(t) \in E_h$, then the trajectory in t is made of a regular point. See below for an illustration.

Definition 4 (Boundary). A boundary in a discrete state d_s is a set of states defined by $e(i, \pi_0, d_s) = \{(\pi, d_s) \in E_h \mid \pi^i = \pi_0\}$, where $i \in \{1, 2, \dots, N\}$, $d_s \in E_d$ and $\pi_0 \in \{0, 1\}$. The boundary $e(i, \pi_0, d_s)$ is inside the discrete state d_s . In the rest of this paper, we simply use e to represent a boundary.

A toy example of HGRN, not based on any real-world biological system, is shown in Figure 2. This example is related to a negative feedback loop with two genes: A (first dimension) and B (second dimension), where A activates B and B inhibits A. Each gene has two discrete levels, so there are four discrete states in this system. Black arrows represent the celerities of each discrete state and red arrows represent a possible trajectory of this system, which happens, in this particular case, to be a closed trajectory.

The state $h_M = ((\pi_M^1, 1), (1, 1))$ of point M belongs to the upper boundary e_1 in the second dimension of the discrete state 11, which is a shorthand notation of $(1, 1)$. Since there is no other discrete state on the other side of e_1 , the trajectory from h_M cannot cross e_1 and has to slide along e_1 . Boundaries like e_1 , which can be reached by trajectories but cannot be crossed, are defined as *attractive boundaries*. If there was another discrete state on the other side of e_1 , in which the celerity is negative in the second dimension (towards the boundary), then the trajectory from h_M could still not cross it, and in this case e_1 would also be an attractive boundary.

The state $h_P = ((\pi_P^1, 0), (0, 1))$ of point P belongs to the lower boundary e_2 in the second dimension of the discrete state 01. The trajectory from h_P will reach instantly $h_Q = ((\pi_Q^1, 1), (0, 0))$, which belongs to the upper boundary e_3 in the second dimension of discrete state 00, because the celerities on both sides allow this (instant) discrete transition. e_2 is defined as an *output boundary* of 01 and e_3 is defined as an *input boundary* of 00.

The trajectory in Figure 2 only reaches one new boundary at a time, however generally a trajectory can reach several new boundaries at the same time.

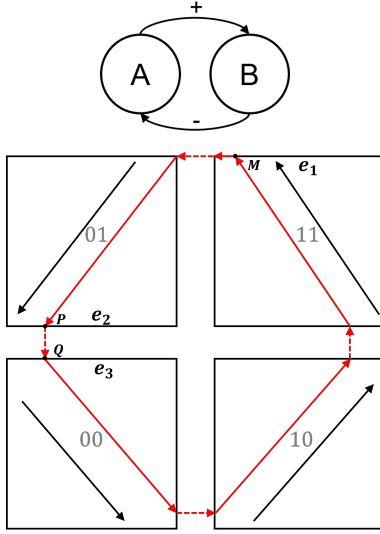


Figure 2: Example of a HGRN of negative feedback loop with 2 genes: gene A and gene B, where A activates B and B inhibits A. Abscissa represents the first gene (gene A) and ordinate represents the second gene (gene B).

When a trajectory reaches several output boundaries at the same time, it can cross any of them but can only cross one boundary at a time, which causes non-deterministic behaviors.

2.2 HGRN of the repressilator

Here we only focus on the influence graph of the canonical repressilator, see Figure 1. We assume that each gene has one threshold when it influences one another gene. Although, *a priori*, one gene can have multiple thresholds for one another gene, in this work we only consider the simplest case. Based on this assumption, since each gene only influences one other gene in this influence graph, it has only two discrete levels separated by only one threshold.

The parameters (celerities) of this HGRN of the repressilator are shown symbolically in Table 1. Each parameter in Table 1 is strictly positive and is denoted by C_{xyzj} , which represents the absolute value of the celerity of variable x when the discrete level of variable y is i and the discrete level of variable z is j . Consider the influence of A on B: when the discrete level of A is 1, meaning that the expression of A is above the threshold to inhibit B, then the temporal derivative of B is always negative, no matter the discrete level of B (0 or 1) which corresponds to the negative values $-C_{ba1b0}$ and $-C_{ba1b1}$. On the other hand, when the expression of A is below the threshold to inhibit B, the temporal derivative of B is always positive, corresponding to parameters C_{ba0b0} and C_{ba0b1} . From the parameters in this table, we can also see that the

number of different parameters (12) is smaller than the multiplication of the number of dimensions by the number of discrete states (24), because some discrete states have celerities in common (same regulation on some variables).

In addition to the threshold which separates the discrete levels 0 and 1, each gene also has a maximal value and a minimal value. For example, when A inhibits B (see Figure 1), B will continue to decrease until it reaches the minimal value (most of the time this minimal value is 0) which is related to the lower boundary in the second dimension (the dimension of gene B) of discrete state 10^* , where $*$ can be 0 or 1. Similarly, when A does not inhibit B, B will continue to increase until it reaches the upper boundary in the second dimension of 01^* .

Table 1: Parameters of the HGRN of the repressilator.

A	B	C	C_A	C_B	C_C
0	0	0	C_{ac0a0}	C_{ba0b0}	C_{cb0c0}
0	0	1	$-C_{ac1a0}$	C_{ba0b0}	C_{cb0c1}
0	1	0	C_{ac0a0}	C_{ba0b1}	$-C_{cb1c0}$
0	1	1	$-C_{ac1a0}$	C_{ba0b1}	$-C_{cb1c1}$
1	0	0	C_{ac0a1}	$-C_{ba1b0}$	C_{cb0c0}
1	0	1	$-C_{ac1a1}$	$-C_{ba1b0}$	C_{cb0c1}
1	1	0	C_{ac0a1}	$-C_{ba1b1}$	$-C_{cb1c0}$
1	1	1	$-C_{ac1a1}$	$-C_{ba1b1}$	$-C_{cb1c1}$

Figure 3 gives two simulations with two different choices of parameters. The simulation on the left represents a sustained oscillation while the simulation on the right represents a damped oscillation. In the simulation on the left, gene C continues to increase from $t = 0$ until it reaches the maximal value, which also means that the trajectory reaches an attractive boundary, then the trajectory will slide along this boundary (called the sliding mode) so that the value of gene C stays unchanged for some time. The sliding mode is an important property of HGRNs.

3 Qualitative behaviors in this HGRN of the repressilator

In this section, we discuss different qualitative properties of this HGRN. To analyze dynamical properties of a HGRN, we need to firstly analyze the transition graph of discrete states, which is determined by the signs of celerities. The signs of celerities of this HGRN of the repressilator can be found in Table 1, based on which the transition graph of discrete states can be constructed using the classical discrete asynchronous semantics, see Figure 4.

From the transition graph, we can see that there

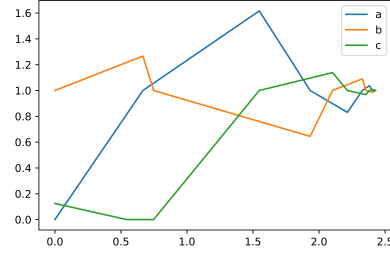
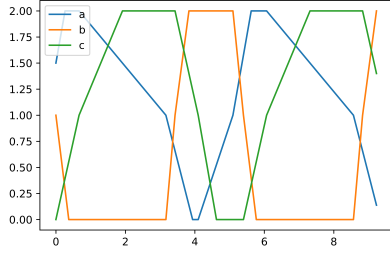


Figure 3: Simulations of the HGRN of the repressilator with two different choices of parameters (Abscissa represents time and ordinate represents the sum of the fractional part and the discrete state of each gene). Parameters of the model on the left: $C_{ac0a0} = 1$, $C_{ac0a1} = 1.9$, $C_{ac1a0} = 1.3$, $C_{ac1a1} = 0.4$, $C_{ba0b0} = 3.8$, $C_{ba0b1} = 2.5$, $C_{ba1b0} = 2.7$, $C_{ba1b1} = 3.3$, $C_{cb0c0} = 1.5$, $C_{cb0c1} = 0.8$, $C_{cb1c0} = 1.9$, $C_{cb1c1} = 1.5$. Parameters of the model on the right: $C_{ac0a0} = 1.5$, $C_{ac0a1} = 0.7$, $C_{ac1a0} = 0.6$, $C_{ac1a1} = 1.6$, $C_{ba0b0} = 2.1$, $C_{ba0b1} = 0.4$, $C_{ba1b0} = 0.3$, $C_{ba1b1} = 3.3$, $C_{cb0c0} = 1.25$, $C_{cb0c1} = 0.25$, $C_{cb1c0} = 0.23$, $C_{cb1c1} = 1.23$.

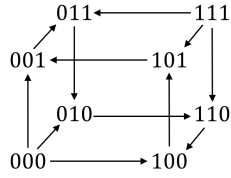


Figure 4: Transition graph of discrete states of the HGRN of the repressilator.

is a unique cycle of discrete states, which is $001 \rightarrow 011 \rightarrow 010 \rightarrow 110 \rightarrow 100 \rightarrow 101 \rightarrow 001$. This cycle is a global attractor of discrete states (the unique terminal strongly connected component), which means that any trajectory in this HGRN will finally enter this cycle.

Following the same sequence of discrete states, there is a special hybrid trajectory: $((1, 1, 0), (0, 0, 1)) \rightarrow ((1, 0, 0), (0, 1, 1)) \rightarrow ((1, 0, 1), (0, 1, 0)) \rightarrow ((0, 0, 1), (1, 1, 0)) \rightarrow ((0, 1, 1), (1, 0, 0)) \rightarrow ((0, 1, 0), (1, 0, 1)) \rightarrow ((1, 1, 0), (0, 0, 1))$. It is illustrated in Figure 5 by green arrows. This trajectory contains 6 different states (the last and the first one are identical). From each state in this trajectory, there is an instant transition (transition which crosses boundaries between discrete states and takes no time), which reaches the next state. This trajectory represents also a closed trajectory, meaning that beginning from each of these 6 states, the trajectory will return to the initial state. When representing trajectories, we often use an embedding of hybrid states in \mathbb{R}^N : a state (π, d_s) is represented in \mathbb{R}^N by summing its discrete and fractional parts: $\pi + d_s$. We say that the hybrid state (π, d_s) and the point $\pi + d_s \in \mathbb{R}^N$ are *related*. When doing so, the six previous hybrid states are embedded in the same point H_0 in \mathbb{R}^3 : $H_0 = (1.0, 1.0, 1.0)$. H_0 is called a *characteristic state* of this HGRN. The characteristic state is formally defined as follows:

Definition 5 (Characteristic state). A *characteristic state* of a HGRN is a state H in the continuous space such that: for any hybrid state h_0 related to H , all trajectories from h_0 will never reach a hybrid state which is not related to H , and there exist oscillations in any small neighborhood of H .

In this paper, we say that a trajectory of a HGRN is an oscillation if it is related to an oscillation in the continuous space. Likewise, the nature of an oscillation of a HGRN (damped or sustained) and the relation between an oscillation and a characteristic state (converging to the characteristic state, moving away from it, etc.) are determined by the related oscillation in the continuous space. A neighborhood of a characteristic state H is defined as a set $\mathcal{N}(H) = \{(\pi, d_s) \in E_h \mid \|\pi + d_s - H\| < r\}$ where $r \in \mathbb{R}$ is the radius of the neighborhood.

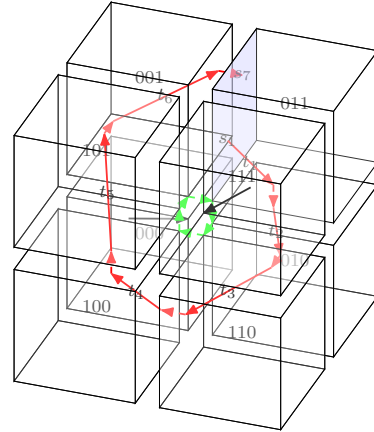


Figure 5: Illustration of the closed trajectory with only instant transitions (green arrows), two special trajectories which can reach directly the characteristic state (black arrows), and a trajectory without sliding mode (red arrows) in this HGRN of the canonical repressilator.

In the continuous space, a characteristic state is a fixed point, because from any hybrid state h related to a characteristic state, all trajectories can only reach hybrid states related to this characteristic state.

We can easily prove that H_0 is a characteristic state: apart from the 6 hybrid states on this closed trajectory, there are two other hybrid states which are related to H_0 : $((1, 1, 1), (0, 0, 0))$ and $((0, 0, 0), (1, 1, 1))$. From each of these two other states, all trajectories reach directly the closed trajectory, and once they do, they can never leave it. Finally, we can find oscillations which follow the unique cycle of discrete states in any neighborhood of H_0 . In this HGRN, there is only one characteristic state. This can be proved by verifying all “corners” of discrete states.

All trajectories in this HGRN will oscillate in this unique cycle of discrete states, except some special trajectories from discrete state 000 or 111 which can reach directly a hybrid state related to the characteristic state, see for example the black arrows in Figure 5. These oscillations can have several different dynamical properties.

To better illustrate the possible dynamical properties in this repressilator, different qualitative behaviors of a HGRN of negative feedback loop in 2 dimensions are illustrated in Figure 6, where black arrows represent celerities in each discrete state and red arrows represent some trajectories. The three figures are obtained by choosing three different parameterisations, which represent the three qualitative behaviors of this HGRN. The closed trajectory with states P, M, N, Q contains only instant transitions. The state in continuous space that is related to states P, M, N, Q is a characteristic state, and is the only characteristic state in this HGRN. On the left, the characteristic state is stable as all trajectories tend to converge to it. In this case, there is no sustained oscillation. On the right, the characteristic state is unstable as all trajectories from a small neighborhood of the characteristic state will move away from it and will finally reach a stable limit cycle containing at least one sliding mode, like the closed trajectory in Figure 2. Between these two cases, in the middle, there is a third possibility in which all trajectories circle around the characteristic state without getting closer or moving away, which we call *parallel cycles* and can be considered as a special case of sustained oscillations.

The HGRN of the repressilator in 3 dimensions (Figure 1) is more complicated than the example HGRN of negative feedback loop in 2 dimensions (Figures 2 and 6), but we think that it also has three similar qualitative behaviors, since each discrete state in the only cycle of discrete states has only one successor (Figure 4). However, we have no proof for the

non-existence of other possibilities yet, for example chaos or the co-existence of sustained oscillations and a stable fixed point. So in this work, we make Hypothesis 1.

Hypothesis 1. *In this HGRN of canonical repressilator (see Figure 1 and Table 1), either the characteristic state is stable and all oscillations are damped, or the characteristic state is unstable and all oscillations are sustained.*

In this HGRN of the canonical repressilator, the characteristic state is said *stable* if we can find a small neighborhood around the characteristic state such that all oscillations which begin from this neighborhood converge to the characteristic state, and the characteristic state is said *unstable* if there is no damped oscillation which converges to it.

Now, based on Hypothesis 1, we can use the stability of the characteristic state to determine the existence of sustained oscillations in this HGRN of the repressilator: all oscillations are sustained if and only if the characteristic state is unstable. This is the main idea used in this work to find conditions for the existence of sustained oscillations. A similar idea was used in other works with differential models, see for example (Page and Perez-Carrasco, 2018; Wang et al., 2006; El Samad et al., 2005).

The problem now is how to analyze the stability of the characteristic state. To do so, we apply a method based on the Poincaré map.

4 Analysis of the Poincaré map

In this section, a method based on the Poincaré map is proposed to compute a sufficient and necessary condition for the existence of sustained oscillations.

4.1 Poincaré map in HGRNs

The Poincaré map was initially proposed to study limit cycles of nonlinear dynamical systems and has also been used later to study limit cycles of hybrid systems (Belgacem et al., 2020; Firippi and Chaves, 2020; Znegui et al., 2020; Flieller et al., 2006; Edwards and Glass, 2005; Girard, 2003; Hiskens, 2001; Edwards, 2000; Mestl et al., 1996). The Poincaré map is the intersection of a periodic orbit with a lower dimension subspace which is called the Poincaré section. The properties of the periodic orbit can be derived from the Poincaré map. In the case of the repressilator studied in this paper, the blue boundary in Figure 5 could be chosen as a Poincaré section.

A method based on the Poincaré map was proposed in (Sun et al., 2022) to analyze the stability of

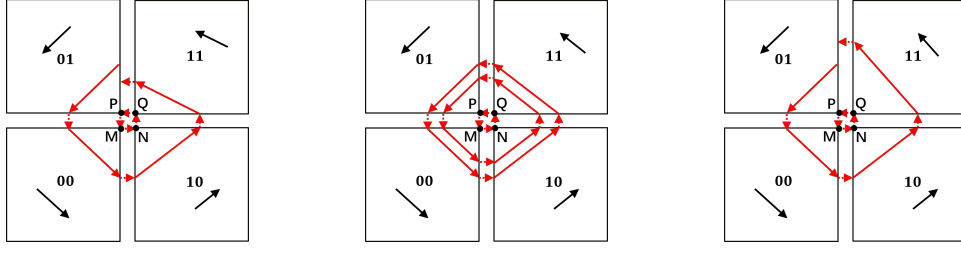


Figure 6: Illustration of different qualitative behaviors in a HGRN of negative feedback loop in 2 dimensions. The three subfigures represent three different choices of parameters.

limit cycles in HGRNs. To illustrate this method, consider another example in 2 dimensions, with an additional discrete level in the first dimension, as shown in Figure 7. In this example, we assume that all parameters (celerities) are known, that is, their real values can directly be used. The upper boundary in the second dimension of discrete state 00 is chosen as Poincaré section. We can see that there is a closed trajectory which intersects this Poincaré section at state $P = (\pi_P, (0,0))$, where $\pi_P \in [0,1]^2$ is the fractional part of state P . We note that in this particular case, $\pi_P = (x,1)$ where $x \in [0,1]$, thus there is only one varying dimension to study in this Poincaré section. According to the properties of HGRNs, we can find on the Poincaré section a neighborhood \mathcal{N} around P , such that trajectory from any state $M = (\pi_M, (0,0))$ from \mathcal{N} will return to the Poincaré section at state $M' = (\pi_{M'}, (0,0))$ and the relation between π_M and $\pi_{M'}$ can be described by an affine matrix application:

$$\pi_{M'} = G(\pi_M) = A\pi_M + b \quad (1)$$

where A is a matrix and b is a vector. We note that the form of Equation (1) is general and applies to any case, including those of dimension higher than 2. At this point, the stability of the closed trajectory depends on the eigenvalues of A . For more details, see (Sun et al., 2022).

In this work, we adapt this method based on the Poincaré map to analyze the stability of the characteristic state, which is a special case of closed trajectory, in order to find conditions for sustained oscillations. As opposed to (Sun et al., 2022) where parameters are assumed to be known, here we compute and analyze symbolically the Poincaré map.

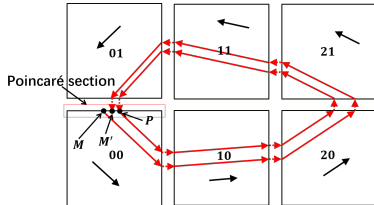


Figure 7: Illustration of the Poincaré map in a HGRN.

4.2 Symbolic Poincaré map

In order to analyze the stability of the characteristic state, we only need to consider trajectories without sliding mode around this state. Indeed, the characteristic state is stable if we can find a small neighborhood around the characteristic state such that all oscillations which begin from this neighborhood converge to the characteristic state. Such a trajectory exists because otherwise, the celerities would prevent the characteristic state from existing. Without loss of generality, we choose the lower boundary in the second dimension of discrete state 011 as Poincaré section; see the blue boundary in Figure 5. Now, we consider any trajectory τ which begins from a state $s_1 = ((x_1, 0, z_1), (0, 1, 1))$ on the Poincaré section and returns to the Poincaré section for the first time at $s_7 = ((x_7, 0, z_7), (0, 1, 1))$ without sliding mode; such a trajectory is illustrated in red in Figure 5. Thus, the Poincaré map is an affine application describing the relation between $(x_1, 0, z_1)$ and $(x_7, 0, z_7)$. Since s_1 is on an input boundary of the discrete state 011, from s_1 , τ will first (continuously) cross the discrete state 011 and reach a state $((x_2, y_2, 0), (0, 1, 1))$ on the lower boundary in the third dimension of 011 which is the output boundary of this discrete state towards 010. We name this output boundary e_1 . Then, it crosses instantly e_1 and reaches an input boundary of 010 in state $((x_2, y_2, 1), (0, 1, 0))$. The duration of crossing in discrete state 011 is:

$$t_1 = \frac{0 - z_1}{-C_{cb1c1}} \quad (2)$$

It should be noted that, to ensure that this trajectory τ has no sliding mode in 011, we also need to ensure that the lower boundary in the first dimension and the upper boundary in the second dimension of 011 are not reached before e_1 , which gives us two additional inequalities:

$$t_1 < \frac{0 - x_1}{-C_{ac1a0}} \quad (3)$$

$$t_1 < \frac{1 - 0}{C_{ba0b1}} \quad (4)$$

In fact, these inequalities can always be satisfied if τ is sufficiently close to the characteristic state, which is the case we consider here. Therefore, in the rest of this section, we do not consider these additional constraints.

Based on the duration t_1 and the fact that there is no sliding mode, we can get the relation between $(x_1, 0, z_1)$ and $(x_2, y_2, 1)$:

$$x_2 = x_1 - C_{ac1a0} \times t_1 \quad (5)$$

$$y_2 = 0 + C_{ba0b1} \times t_1 \quad (6)$$

Following the same process, we can get the duration of τ in each discrete state and the relations between states from one input boundary to another input boundary:

$$t_2 = \frac{1-x_2}{C_{ac0a0}} \quad t_3 = \frac{0-y_3}{-C_{ba1b1}} \quad t_4 = \frac{1-z_4}{C_{cb0c0}} \quad (7)$$

$$t_5 = \frac{0-x_5}{-C_{ac1a1}} \quad t_6 = \frac{1-y_6}{C_{ba0b0}} \quad (8)$$

$$y_3 = y_2 + C_{ba0b1} \times t_2 \quad z_3 = 1 - C_{cb1c0} \times t_2 \quad (9)$$

$$x_4 = 0 + C_{ac0a1} \times t_3 \quad z_4 = z_3 - C_{cb1c0} \times t_3 \quad (10)$$

$$x_5 = x_4 + C_{ac0a1} \times t_4 \quad y_5 = 1 - C_{ba1b0} \times t_4 \quad (11)$$

$$y_6 = y_5 - C_{ba1b0} \times t_5 \quad z_6 = 0 + C_{cb0c1} \times t_5 \quad (12)$$

$$x_7 = 1 - C_{ac1a0} \times t_6 \quad z_7 = z_6 + C_{cb0c1} \times t_6 \quad (13)$$

where t_2, t_3, t_4, t_5, t_6 are the durations of τ in discrete states 010, 110, 100, 101, 001 respectively, and $(0, y_3, z_3), (x_4, 1, z_4), (x_5, y_5, 0), (1, y_6, z_6), (x_7, 0, z_7)$ are the fractional parts of the states when τ first reaches 110, 100, 101, 001, 011 respectively.

Based on the above equations, the Poincaré map can be calculated to describe the relation between $(x_1, 0, z_1)$ and $(x_7, 0, z_7)$ as follows. One dimension is missing in the matrix below; indeed, this dimension is useless in the computation of the stability, for more details see (Sun et al., 2022).

$$\begin{pmatrix} x_7 \\ z_7 \end{pmatrix} = \begin{bmatrix} b_1 & c_1 \\ b_2 & c_2 \end{bmatrix} \begin{pmatrix} x_1 \\ z_1 \end{pmatrix} + \begin{pmatrix} a_1 \\ a_2 \end{pmatrix} \quad (14)$$

In the above equation, $a_1, a_2, b_1, b_2, c_1, c_2$ are nonlinear combinations of the celerity values. Their expressions are given in the appendix. We can easily derive that b_1 and c_2 are strictly positive, while b_2 and c_1 are strictly negative.

4.3 Analysis of eigenvalues

The stability of the characteristic state depends on the two eigenvalues of $\begin{bmatrix} b_1 & c_1 \\ b_2 & c_2 \end{bmatrix}$, which are:

$$\lambda_1 = \frac{b_1 + c_2 + \sqrt{(b_1 - c_2)^2 + 4c_1b_2}}{2} \quad (15)$$

$$\lambda_2 = \frac{b_1 + c_2 - \sqrt{(b_1 - c_2)^2 + 4c_1b_2}}{2} \quad (16)$$

Property 1. These two eigenvalues are real and strictly positive.

Proof. From the expressions of b_1, b_2, c_1, c_2 , we know that $b_1 > 0, b_2 < 0, c_1 < 0, c_2 > 0$, so we have $(b_1 - c_2)^2 + 4c_1b_2 > 0$, therefore these two eigenvalues are real. Moreover, the expression of the product of these two eigenvalues is:

$$\lambda_1 \times \lambda_2 = b_1c_2 - c_1b_2 = \frac{D_{\lambda_1 \times \lambda_2}}{D_0} \quad (17)$$

where

$$D_{\lambda_1 \times \lambda_2} = C_{ac0a1}C_{ac1a0}C_{ba0b1}C_{ba1b0}C_{cb0c1}C_{cb1c0} \quad (18)$$

$$D_0 = C_{ac0a0}C_{ac1a1}C_{ba0b0}C_{ba1b1}C_{cb0c0}C_{cb1c1} \quad (19)$$

Therefore, $\lambda_1 \times \lambda_2 > 0$. Since λ_1 is strictly positive, so is λ_2 . \square

Suppose that two eigenvectors which are related to λ_1 and λ_2 respectively are $v_1 = (v_1^1, v_1^2)$ and $v_2 = (v_2^1, v_2^2)$. We have the following property on v_1 and v_2 .

Property 2. $v_1^1 \times v_1^2 < 0$ and $v_2^1 \times v_2^2 > 0$.

Proof. Since v_1 is a eigenvector related to λ_1 , we have:

$$\lambda_1 \begin{pmatrix} v_1^1 \\ v_1^2 \end{pmatrix} = \begin{bmatrix} b_1 & c_1 \\ b_2 & c_2 \end{bmatrix} \begin{pmatrix} v_1^1 \\ v_1^2 \end{pmatrix} \quad (20)$$

From which, we have:

$$v_1^2 = \frac{\lambda_1 - b_1}{c_1} v_1^1 \quad (21)$$

By developing the expression $\frac{\lambda_1 - b_1}{c_1}$, we have:

$$\frac{\lambda_1 - b_1}{c_1} = \frac{c_2 - b_1 + \sqrt{(c_2 - b_1)^2 + 4c_1b_2}}{2c_1} \quad (22)$$

We can see that whether $c_2 - b_1$ is positive or negative, $\lambda_1 - b_1$ is always strictly positive because $|c_2 - b_1| < \sqrt{(c_2 - b_1)^2 + 4c_1b_2}$. Since c_1 is strictly negative, we have $v_1^1 \times v_1^2 < 0$.

Similarly for v_2 , we can have:

$$v_2^2 = \frac{\lambda_2 - b_1}{c_1} v_2^1 \quad (23)$$

and

$$\frac{\lambda_2 - b_1}{c_1} = \frac{c_2 - b_1 - \sqrt{(c_2 - b_1)^2 + 4c_1b_2}}{2c_1} \quad (24)$$

So, similarly, whether $c_2 - b_1$ is positive or negative, $\lambda_2 - b_1$ is always strictly negative. And since c_1 is strictly negative, we have $v_2^1 \times v_2^2 > 0$. \square

Based on these properties, we develop the following theorem to verify the stability of the characteristic state.

Theorem 1. *The characteristic state is unstable if and only if $\lambda_1 \geq 1$.*

Proof. For any trajectory τ sufficiently close to the characteristic state but different from the characteristic state, which reaches the chosen Poincaré section at a state $s = ((x_1, 0, z_1), (0, 1, 1))$, and then reaches this Poincaré section again for the first time at another state $s' = ((x_2, 0, z_2), (0, 1, 1))$, such that there is no sliding mode between s and s' , since the state $((1, 0, 0), (0, 1, 1))$ (which is related to the characteristic state) is a fixed point of the Poincaré map, we can have the following relation:

$$\begin{pmatrix} x'_2 \\ z'_2 \end{pmatrix} = \begin{bmatrix} b_1 & c_1 \\ b_2 & c_2 \end{bmatrix} \begin{pmatrix} x'_1 \\ z'_1 \end{pmatrix} \quad (25)$$

where (x'_1, z'_1) and (x'_2, z'_2) are the new coordinates of (x_1, z_1) and (x_2, z_2) by taking $(1, 0)$ as the new origin, which means that $x'_i = x_i - 1$, $z'_i = z_i - 0$, where $i \in \{1, 2\}$. In fact, this change of coordinates allows to remove the affine vector b , as opposed to the general form given in Equation (1).

Vectors (x'_1, z'_1) and (x'_2, z'_2) can be decomposed by:

$$\begin{pmatrix} x'_1 \\ z'_1 \end{pmatrix} = \alpha_1 v_1 + \beta_1 v_2 \quad (26)$$

$$\begin{pmatrix} x'_2 \\ z'_2 \end{pmatrix} = \alpha_2 v_1 + \beta_2 v_2 \quad (27)$$

where $\alpha_1, \beta_1, \alpha_2, \beta_2 \in \mathbb{R}$ and α_1 is not null as $x'_1 < 0$, $z'_1 > 0$, $v_1^1 \times v_1^2 < 0$ and $v_2^1 \times v_2^2 > 0$.

By multiplying Equation (26) on the left by $\begin{bmatrix} b_1 & c_1 \\ b_2 & c_2 \end{bmatrix}$ and from Equation (25), we can derive that:

$$\alpha_2 = \lambda_1 \alpha_1 \quad (28)$$

$$\beta_2 = \lambda_2 \beta_1 \quad (29)$$

Consider the case where $\lambda_1 \geq 1$. Since $|\alpha_1|$ is strictly positive, then we have $|\alpha_2| \geq |\alpha_1|$, which means that s' is not closer to the characteristic state than s in the direction of v_1 . Therefore, any sequence of the intersection points of τ with this Poincaré section will never converge to the characteristic state, which indicates that the characteristic state is unstable. This proves that “the characteristic state is unstable” is a necessary condition for “ $\lambda_1 \geq 1$ ”.

Now consider the case where the characteristic state is unstable, meaning that there is no damped oscillation that converges to it. We suppose that $\lambda_1 < 1$. Since $\lambda_1 > \lambda_2 > 0$, we have $|\alpha_2| < |\alpha_1|$ and $|\beta_2| < |\beta_1|$, which means that if τ is sufficiently close to the

characteristic state, then it converges to the characteristic state, which contradicts the hypothesis stating that the characteristic state is unstable. This proves that “the characteristic state is unstable” is a sufficient condition for “ $\lambda_1 \geq 1$ ”. \square

Based on Hypothesis 1 and Theorem 1, the condition $\lambda_1 \geq 1$ is a sufficient and necessary condition for the existence of sustained oscillations in this HGRN of canonical repressilator.

Since our final objective is to provide practical information for the construction of synthetic networks, conditions like $\lambda_1 \geq 1$ might not be a good result, because the set of models under this constraint is not easy to figure. In the next section, a method to compute separable constraints based on the condition $\lambda_1 \geq 1$ is presented.

5 Computation of sufficient separable constraints on parameters

In this section, we propose a method to compute separable constraints on parameters based on the condition $\lambda_1 \geq 1$ which is developed in the previous section. In this paper, separable constraints mean constraints with separable form: each parameter is constrained by an interval, for example $C_{ac0a0} \in [\underline{C_{ac0a0}}, \overline{C_{ac0a0}}]$. In other words, these separable constraints represent a n -dimensional bounding box in the space of parameters (celerities). What we want to do is to find such a n -dimensional box so that any model in this bounding box satisfies the condition $\lambda_1 \geq 1$, which means that any model in this box has sustained oscillations.

Firstly, we present a simplification of the condition $\lambda_1 \geq 1$. Secondly, we introduce a method to verify if all models in a given bounding box satisfy this simplified condition. At last, using the method in the second part, we propose a search algorithm to find some separable constraints.

5.1 Condition simplification

The condition:

$$\lambda_1 = \frac{b_1 + c_2 + \sqrt{(b_1 - c_2)^2 + 4c_1b_2}}{2} \geq 1 \quad (30)$$

can be reformulated as:

$$b_1 + c_2 - 2 \geq -\sqrt{(b_1 - c_2)^2 + 4c_1b_2} \quad (31)$$

which is equivalent to:

$$\begin{aligned} & (b_1 + c_2 - 2 \geq 0) \vee \\ & ((b_1 + c_2 - 2 < 0) \wedge \\ & ((b_1 + c_2 - 2)^2 \leq (b_1 - c_2)^2 + 4c_1b_2)) \end{aligned} \quad (32)$$

or:

$$(b_1 + c_2 - 2 \geq 0) \vee (b_1c_2 - c_1b_2 - b_1 - c_2 + 1 \leq 0) \quad (33)$$

This last condition is equivalent to $(P_1 \geq 0) \vee (P_2 \geq 0)$ where P_1 and P_2 are polynomials on parameters. The expressions of P_1 and P_2 are given in the appendix.

Condition $(P_1 \geq 0) \vee (P_2 \geq 0)$ seems preferable to $\lambda_1 \geq 1$ because it only contains polynomials. In fact, one can easily prove that solutions for $(P_1 \geq 0) \vee (P_2 \geq 0)$ exist. For example, by only considering $Cac0a0$ and $Cac0a1$, which are two parameters describing the derivative of gene A when gene C does not inhibit gene A , P_1 and P_2 can be expressed by:

$$\begin{aligned} P_1 = & p_{11} \times Cac0a0 + p_{12} \times Cac0a1 \\ & + p_{13} \times Cac0a0 \times Cac0a1 + p_{14} \end{aligned} \quad (34)$$

$$\begin{aligned} P_2 = & p_{21} \times Cac0a0 + p_{22} \times Cac0a1 \\ & + p_{23} \times Cac0a0 \times Cac0a1 + p_{24} \end{aligned} \quad (35)$$

where p_{ij} (with $i \in \{1, 2\}$, $j \in \{1, 2, 3, 4\}$) are expressions of parameters which do not include $Cac0a0$ and $Cac0a1$. We can see that if $Cac0a0$ and $Cac0a1$ converge to 0 while other parameters remain unchanged, P_1 and P_2 converge to p_{14} and p_{24} respectively, which are both positive. This indicates that the solutions of $(P_1 \geq 0) \vee (P_2 \geq 0)$ exist and also implies a new control strategy for the existence of sustained oscillations: controlling the derivatives of gene A when A is not inhibited by C such that these derivatives are sufficiently small, while keeping other parameters unchanged.

5.2 Satisfiability under separable constraints

In this subsection, we adapt the range enclosure property of Bernstein coefficients to verify if all models in a given bounding box satisfy the condition $(P_1 \geq 0) \vee (P_2 \geq 0)$. The Bernstein coefficients have been used in the literature to, for example, compute images for polynomial dynamical system (Dang and Salinas, 2009; Dang and Testylier, 2012), or compute affine lower bound functions for polynomials (Garloff and Smith, 2003), etc.

Before introducing the Bernstein coefficients, we firstly introduce the notion of multi-indices. A multi-index is a vector of non-negative integers. Given two multi-indices $i = (i_1, i_2, \dots, i_n)$ and $j = (j_1, j_2, \dots, j_n)$,

we write $i \leq j$ if $\forall k \in \{1, 2, \dots, n\}$, $i_k \leq j_k$. We also write $\frac{i}{j}$ for $(\frac{i_1}{j_1}, \frac{i_2}{j_2}, \dots, \frac{i_n}{j_n})$ and $\binom{j}{i}$ for $\binom{j_1}{i_1} \binom{j_2}{i_2} \dots \binom{j_n}{i_n}$ which is the multiplication of all binomial coefficient $\binom{j_k}{i_k}$, $k \in \{1, 2, \dots, n\}$.

Using the multi-indices, a polynomial $f: \mathbb{R}^n \rightarrow \mathbb{R}$ can be represented as follows:

$$f(x) = \sum_{i \in I_d} a_i x^i \quad (36)$$

where $a_i \in \mathbb{R}$, i and d are multi-indices, I_d is set of all multi-indices i such that $i \leq d$, and $x^i = x_1^{i_1} x_2^{i_2} \dots x_n^{i_n}$ which is the product of all $x_j^{i_j}$, where x_j is the j^{th} variable of polynomial f .

f can also be expressed by Bernstein expansion as follows:

$$f(x) = \sum_{i \in I_d} b_i \mathcal{B}_{d,i}(x) \quad (37)$$

where

$$\mathcal{B}_{d,i}(x) = \beta_{d_1,i_1}(x_1) \dots \beta_{d_n,i_n}(x_n) \quad (38)$$

$$\beta_{d_k,i_k}(x_k) = \binom{d_k}{i_k} x_k^{i_k} (1 - x_k)^{d_k - i_k} \quad (39)$$

$$b_i = \sum_{j \leq i} \binom{i}{j} \frac{a_j}{\binom{d}{j}} \quad (40)$$

where d and i are multi-indices and $k \in \{1, 2, \dots, n\}$. The values b_i , for $i \in I_d$ are called Bernstein coefficients.

One fundamental property of Bernstein coefficients for our approach is the range enclosure property, which can be derived from the convex hull property. The convex hull of a set S , noted $\text{Conv}(S)$, is the smallest convex set that contains S .

Lemma 1 (Convex hull property). $\text{Conv}\{(x, f(x)) \mid x \in B\} \subseteq \text{Conv}\{(i/d, b_i) \mid i \in I_d\}$.

Lemma 2 (Range enclosure property). $\min\{b_i \mid i \in I_d\} \leq f(x) \leq \max\{b_i \mid i \in I_d\}$, $\forall x \in B$, where $B = [0, 1]^n$ is the unit box.

The range enclosure property over-approximates the range of image of f on B and can be used to verify if all models in a given bounding box satisfy the condition $(P_1 \geq 0) \vee (P_2 \geq 0)$. To do so, we need to firstly make a change of variables of polynomials P_1 and P_2 , such that all variables are included in $[0, 1]$. For example, the variable $Cac0a0 \in [\underline{Cac0a0}, \overline{Cac0a0}]$ is replaced by $Cac0a0 = (\overline{Cac0a0} - \underline{Cac0a0}) \times X_{ac0a0} + \underline{Cac0a0}$, where $X_{ac0a0} \in [0, 1]$. By doing so, we get two new polynomials P'_1 and P'_2 .

So now, to verify if $(P_1 \geq 0) \vee (P_2 \geq 0)$ is always true in a given bounding box, we only need to verify if $(P'_1 \geq 0) \vee (P'_2 \geq 0)$ is always true in the unit box. To do so, we compute the Bernstein coefficients $\{b_{1,i}\}$ and $\{b_{2,i}\}$ (where $i \in I_d$) of P'_1 and P'_2 respectively. A sufficient condition for the condition “ $(P'_1 \geq 0) \vee (P'_2 \geq 0)$ is always true in the unit box” (condition1) is “ $(\forall i \in I_d, b_{1,i} \geq 0) \vee (\forall i \in I_d, b_{2,i} \geq 0)$ ” (condition2), according to the range enclosure property. In fact, since the minimum value of the image of P'_1 on the unit box is always larger or equal to the minimum value of $\{b_{1,i}\}$, “ $\{b_{1,i}\}$ are not negative” ($\forall i \in I_d, b_{1,i} \geq 0$) indicates that “ P'_1 are not negative on the unit box”, and the same holds for P'_2 . Since there is a finite number of Bernstein coefficients, condition2 can be verified. Therefore, in this work, condition2 is used to verify if all models in a given bounding box always have sustained oscillations.

5.3 Search of separable constraints

Based on the method introduced in the previous subsection, we propose a depth first algorithm to find some bounding boxes which satisfy condition2. This algorithm is illustrated in Figure 8. Initially, each parameter is included in an interval. In this implementation, without loss of generality, we assume that each parameter is included initially in $[0, 1]$. Then, we verify if condition2 is satisfied for this bounding box using the method proposed in the previous subsection. If it is satisfied, then it is a bounding box such that all models in it have sustained oscillations. If condition2 is not satisfied, then there might be some models in this bounding box which do not have sustained oscillations, in this case the bounding box is split into two smaller bounding boxes (by splitting the largest interval into two) which have the same volume and the process is repeated on each of these two new bounding boxes. Each path in this algorithm will stop, either when a bounding box which satisfies condition2 is found or when the length of the largest interval is smaller than a certain threshold. In fact, similar ideas are widely used to find solution sets under non-linear constraints (Ziat et al., 2019; Pelleau et al., 2013).

Since the HGRN of the canonical repressilator has 12 parameters (see Table 1), and if we assume that the number of possible smallest intervals for each parameter are the same, noted m , then there are at most m^{12} smallest bounding boxes to check. Verifying all these boxes can be time consuming. In our implementation, we assume that the intervals of these three genes are identical, which means that we search for bounding boxes such that $\overline{C_{aciaj}} = \overline{C_{baibj}} = \overline{C_{cbicj}}$ and $\underline{C_{aciaj}} = \underline{C_{baibj}} = \underline{C_{cbicj}}$ for any $i, j \in \{0, 1\}$, where, for

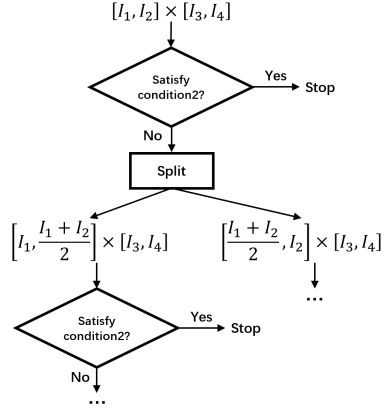


Figure 8: Illustration of the algorithm to search for some bounding boxes.

example, $[\underline{C_{ac0a0}}, \overline{C_{ac0a0}}]$ is the interval of the parameter C_{ac0a0} , so that we only need to consider 4 independent intervals when searching for bounding boxes. This assumption is only applied here to decrease the number of possible bounding boxes. Similar assumption about the symmetry between these three genes was also made in works based on differential equations, see for example (Buşe et al., 2010). We also assume that the minimal length of interval is greater or equal to 0.5. A value smaller than 0.5 could naturally be chosen, but this might exponentially increase the number of possible bounding boxes, which could also exponentially increase the execution time. With these assumptions, we obtain 5 bounding boxes which satisfy the condition2. In the results below, (y, x) represents (c, a) , (a, b) and (b, c) , where y inhibits x , for example C_{xy0x0} presents C_{ac0a0} , C_{ba0b0} and C_{cb0c0} .

Bounding box 1: $C_{xy0x0} \in [0, 0.5], C_{xy0x1} \in [0, 0.5], C_{xy1x0} \in [0.5, 1], C_{xy1x1} \in [0, 1]$

Bounding box 2: $C_{xy0x0} \in [0, 0.5], C_{xy0x1} \in [0.5, 1], C_{xy1x0} \in [0, 0.5], C_{xy1x1} \in [0, 0.5]$

Bounding box 3: $C_{xy0x0} \in [0, 0.5], C_{xy0x1} \in [0.5, 1], C_{xy1x0} \in [0.5, 1], C_{xy1x1} \in [0, 1]$

Bounding box 4: $C_{xy0x0} \in [0.5, 1], C_{xy0x1} \in [0.5, 1], C_{xy1x0} \in [0, 0.5], C_{xy1x1} \in [0, 0.5]$

Bounding box 5: $C_{xy0x0} \in [0.5, 1], C_{xy0x1} \in [0.5, 1], C_{xy1x0} \in [0, 0.5], C_{xy1x1} \in [0, 1]$

We can see that these constraints are easy to interpret and some intuitive results can be derived from them: for instance, from Bounding box 2, we can get that sustained oscillations exist if the values of C_{xy0x1} are close to each other and are sufficiently larger than any C_{xy0x0} , C_{xy1x0} and C_{xy1x1} .

6 CONCLUSIONS

In this work, a HGRN of the canonical repressilator is constructed. By computing and analyzing analytically a Poincaré map and based on a hypothesis, a sufficient and necessary condition for the existence of sustained oscillations is developed. Then the range enclosure property of Bernstein coefficients is adapted to find some bounding boxes in parameters space which satisfy this sufficient and necessary condition. These bounding boxes (intervals of parameters) can provide useful information for the design of synthetic circuits. Moreover, an intermediate result implies some new control strategies for sustained oscillations: controlling the absolute values of the derivatives of one gene under certain regulation such that these values are sufficiently small, while keeping other parameters of the system unchanged.

Naive assumptions about the bounding boxes are made in this work. For example, we assume that the influence between these three genes are symmetrical. In other words, some groups of parameters (such as C_{ac0a0} , C_{ba0b0} and C_{cb0c0}) are constrained by the same intervals. These assumptions could be replaced by more realistic ones with access to more biological knowledge. For instance, knowing the intervals of possible values for some parameters would allow to speed up the enumeration of the bounding boxes.

Only the canonical repressilator with three components is considered in this work. This method could be extended for more complex influence graphs that exist in the literature (Page, 2019; Perez-Carrasco et al., 2018; Goh et al., 2008). However, for more complex influence graphs, conditions for the existence of sustained oscillations can be harder to develop, as there could be several cycles of discrete states around one characteristic state: in such a case, one would have to consider the disjunction of the conditions associated with each cycle. It is also possible to extend this work to find condition for other dynamical properties expressed with temporal logics.

In this work, constraints are obtained based on given dynamical properties. In future works, the converse approach might be considered, that is, given a bounding box of parameters, predict possible behaviors of the system.

ACKNOWLEDGEMENTS

We would like to thank Gilles Bernot and Thao Dang for their fruitful discussions.

This work is partly supported by China Scholarship Council.

ADDITIONAL INFORMATION

The code of this work is available at https://github.com/Honglu42/HGRN_repressilator.

REFERENCES

- Batt, G., Belta, C., and Weiss, R. (2007). Model checking genetic regulatory networks with parameter uncertainty. In *International Workshop on Hybrid Systems: Computation and Control*, pages 61–75. Springer.
- Behaegel, J., Comet, J.-P., Bernot, G., Cornillon, E., and Delaunay, F. (2016). A hybrid model of cell cycle in mammals. *Journal of bioinformatics and computational biology*, 14(01):1640001.
- Belgacem, I., Gouzé, J.-L., and Edwards, R. (2020). Control of negative feedback loops in genetic networks. In *2020 59th IEEE Conference on Decision and Control (CDC)*, pages 5098–5105. IEEE.
- Buşe, O., Kuznetsov, A., and Pérez, R. A. (2009). Existence of limit cycles in the repressilator equations. *International Journal of Bifurcation and Chaos*, 19(12):4097–4106.
- Buşe, O., Pérez, R., and Kuznetsov, A. (2010). Dynamical properties of the repressilator model. *Physical Review E*, 81(6):066206.
- Chaves, M. and Gouzé, J.-L. (2011). Exact control of genetic networks in a qualitative framework: the bistable switch example. *Automatica*, 47(6):1105–1112.
- Chaves, M. and Jong, H. d. (2021). Qualitative modeling, analysis and control of synthetic regulatory circuits. *Synthetic Gene Circuits*, pages 1–40.
- Cornillon, E., Comet, J.-P., Bernot, G., and Enée, G. (2016). Hybrid gene networks: a new framework and a software environment. *advances in Systems and Synthetic Biology*.
- Dang, T. and Salinas, D. (2009). Image computation for polynomial dynamical systems using the bernstein expansion. In *International Conference on Computer Aided Verification*, pages 219–232. Springer.
- Dang, T. and Testylier, R. (2012). Reachability analysis for polynomial dynamical systems using the bernstein expansion. *Reliab. Comput.*, 17(2):128–152.
- De Jong, H., Geiselman, J., Hernandez, C., and Page, M. (2003). Genetic network analyzer: qualitative simulation of genetic regulatory networks. *Bioinformatics*, 19(3):336–344.
- Dilão, R. (2014). The regulation of gene expression in eukaryotes: bistability and oscillations in repressilator models. *Journal of theoretical biology*, 340:199–208.
- Dukarić, M., Errami, H., Jerala, R., Lebar, T., Romanovski, V. G., Tóth, J., and Weber, A. (2019). On three genetic repressilator topologies. *Reaction Kinetics, Mechanisms and Catalysis*, 126(1):3–30.
- Edwards, R. (2000). Analysis of continuous-time switching networks. *Physica D: Nonlinear Phenomena*, 146(1-4):165–199.

- Edwards, R. and Glass, L. (2005). A calculus for relating the dynamics and structure of complex biological networks. *Adventures in Chemical Physics: A Special Volume of Advances in Chemical Physics*, 132:151–178.
- El Samad, H., Del Vecchio, D., and Khammash, M. (2005). Repressilators and promotilators: Loop dynamics in synthetic gene networks. In *Proceedings of the 2005, American Control Conference, 2005.*, pages 4405–4410. IEEE.
- Elowitz, M. B. and Leibler, S. (2000). A synthetic oscillatory network of transcriptional regulators. *Nature*, 403(6767):335–338.
- Firippi, E. and Chaves, M. (2020). Topology-induced dynamics in a network of synthetic oscillators with piecewise affine approximation. *Chaos: An Interdisciplinary Journal of Nonlinear Science*, 30(11):113128.
- Flieller, D., Riedinger, P., and Louis, J.-P. (2006). Computation and stability of limit cycles in hybrid systems. *Nonlinear Analysis: Theory, Methods & Applications*, 64(2):352–367.
- Garloff, J. and Smith, A. P. (2003). A comparison of methods for the computation of affine lower bound functions for polynomials. In *International Workshop on Global Optimization and Constraint Satisfaction*, pages 71–85. Springer.
- Girard, A. (2003). Computation and stability analysis of limit cycles in piecewise linear hybrid systems. *IFAC Proceedings Volumes*, 36(6):181–186.
- Goh, K.-I., Kahng, B., and Cho, K.-H. (2008). Sustained oscillations in extended genetic oscillatory systems. *Biophysical Journal*, 94(11):4270–4276.
- Hiskens, I. A. (2001). Stability of hybrid system limit cycles: Application to the compass gait biped robot. In *Proceedings of the 40th IEEE Conference on Decision and Control (Cat. No. 01CH37228)*, volume 1, pages 774–779. IEEE.
- Kuznetsov, A. and Afraimovich, V. (2012). Heteroclinic cycles in the repressilator model. *Chaos, Solitons & Fractals*, 45(5):660–665.
- Mestl, T., Lemay, C., and Glass, L. (1996). Chaos in high-dimensional neural and gene networks. *Physica D: Nonlinear Phenomena*, 98(1):33–52.
- Müller, S., Hofbauer, J., Endler, L., Flamm, C., Widder, S., and Schuster, P. (2006). A generalized model of the repressilator. *Journal of mathematical biology*, 53(6):905–937.
- Page, K. M. (2019). Oscillations in well-mixed, deterministic feedback systems: Beyond ring oscillators. *Journal of Theoretical Biology*, 481:44–53.
- Page, K. M. and Perez-Carrasco, R. (2018). Degradation rate uniformity determines success of oscillations in repressive feedback regulatory networks. *Journal of the Royal Society Interface*, 15(142):20180157.
- Pelleau, M., Miné, A., Truchet, C., and Benhamou, F. (2013). A constraint solver based on abstract domains. In *International Workshop on Verification, Model Checking, and Abstract Interpretation*, pages 434–454. Springer.
- Perez-Carrasco, R., Barnes, C. P., Schaerli, Y., Isalan, M., Briscoe, J., and Page, K. M. (2018). Combining a toggle switch and a repressilator within the ac-dc circuit generates distinct dynamical behaviors. *Cell systems*, 6(4):521–530.
- Potvin-Trottier, L., Lord, N. D., Vinnicombe, G., and Paulson, J. (2016). Synchronous long-term oscillations in a synthetic gene circuit. *Nature*, 538(7626):514–517.
- Sun, H., Folschette, M., and Magnin, M. (2022). Limit cycle analysis of a class of hybrid gene regulatory networks. In *International Conference on Computational Methods in Systems Biology*, pages 217–236. Springer.
- Thomas, R. (1973). Boolean formalization of genetic control circuits. *Journal of theoretical biology*, 42(3):563–585.
- Thomas, R. (1991). Regulatory networks seen as asynchronous automata: a logical description. *Journal of theoretical biology*, 153(1):1–23.
- Wang, R., Chen, L., and Aihara, K. (2006). Construction of genetic oscillators with interlocked feedback networks. *Journal of theoretical biology*, 242(2):454–463.
- Ziat, G., Maréchal, A., Pelleau, M., Miné, A., and Truchet, C. (2019). Combination of boxes and polyhedra abstractions for constraint solving. In *International Symposium on Formal Methods*, pages 119–135. Springer.
- Znegui, W., Gritli, H., and Belghith, S. (2020). Design of an explicit expression of the poincaré map for the passive dynamic walking of the compass-gait biped model. *Chaos, Solitons & Fractals*, 130:109436.

APPENDIX

Supplementary information about the Poincaré map

$$b_1 = \frac{B_1}{D_0} \quad (41)$$

$$b_2 = \frac{B_2}{D_0} \quad (42)$$

$$c_1 = \frac{C_1}{D_0} \quad (43)$$

$$c_2 = \frac{C_2}{D_0} \quad (44)$$

$$\begin{aligned} B_1 = & C_{ac0a1}C_{ac1a0}C_{ba0b1}C_{ba1b0}C_{cb0c0}C_{cb1c1} \\ & + C_{ac0a1}C_{ac1a0}C_{ba0b1}C_{ba1b0}C_{cb1c0}C_{cb1c1} \\ & + C_{ac0a1}C_{ac1a0}C_{ba1b0}C_{ba1b1}C_{cb1c0}C_{cb1c1} \\ & + C_{ac1a0}C_{ac1a1}C_{ba0b1}C_{ba1b0}C_{cb1c0}C_{cb1c1} \\ & + C_{ac1a0}C_{ac1a1}C_{ba1b0}C_{ba1b1}C_{cb1c0}C_{cb1c1} \end{aligned} \quad (45)$$

